J. Chem. Thermodynamics 115 (2017) 191–201

Contents lists available at ScienceDirect

J. Chem. Thermodynamics

journal homepage: www.elsevier.com/locate/jct

Primary and secondary aqueous two-phase systems composed of thermo switchable polymers and bio-derived ionic liquids

Cher Pin Song [a], Ramakrishnan Nagasundara Ramanan [a,b], R. Vijayaraghavan [c], Douglas R. MacFarlane [c], Eng-Seng Chan [a], João A.P. Coutinho [d], Luis Fernandez [d,e], Chien-Wei Ooi [a,b,*]

[a] Chemical Engineering Discipline, School of Engineering, Monash University Malaysia, Jalan Lagoon Selatan, 47500 Bandar Sunway, Selangor, Malaysia
[b] Tropical Medicine and Biology Platform, School of Science, Monash University Malaysia, Jalan Lagoon Selatan, 47500 Bandar Sunway, Selangor, Malaysia
[c] School of Chemistry, Faculty of Science, Monash University, Clayton, VIC 3800, Australia
[d] CICECO – Aveiro Institute of Materials, Department of Chemistry, University of Aveiro, 3810-193 Aveiro, Portugal
[e] Laboratorio de Termodinamica y Fisicoquímica de Fluidos, 35071-Parque Científico-Tecnologico, Universidad de Las Palmas de Gran Canaria, Canary Islands, Spain

ARTICLE INFO

Article history:
Received 12 August 2016
Received in revised form 6 July 2017
Accepted 25 July 2017
Available online 27 July 2017

Keywords:
Liquid-liquid equilibrium
Cholinium aminoate
Poly(propylene glycol)
Thermodynamics
Lower critical solution temperature
Secondary aqueous two-phase system

ABSTRACT

The liquid-liquid equilibrium (LLE) data for aqueous two-phase systems (ATPSs) comprising poly(propylene glycol) 400 (PPG 400) and cholinium-aminoate-based ([Ch][AA]) ionic liquid were determined experimentally at T = (288.15 and 308.15) K, while the LLE data at T = 298.15 K was adopted from our previous work for comparison. The experimental binodal data were satisfactorily fitted to a temperature-dependent nonlinear empirical expression. The reliability of tie-line data was confirmed by fitting the experimental data with the Othmer-Tobias and Bancroft equations. Furthermore, for the first time, the electrolyte nonrandom two-liquid model (e-NRTL) was used to correlate the tie-line data of PPG 400 + [Ch][AA] + water systems. The correlations of LLE data using these models provide a good description of the experimental values. The effect of temperature on the phase-forming capabilities of the corresponding [Ch][AA] was assessed using the experimental binodal data and the salting-out coefficient (k_2) derived from the Setschenow-type equation. The values of k_2 were well correlated to the phase-forming abilities of [Ch][AA], and were found to increase at higher temperature. Upon heating to 308.15 K, the solution of (PPG 400)-rich top phase from the primary PPG 400 + [Ch][AA] + water systems formed the secondary ATPSs. The LLE data of the secondary PPG 400 + [Ch][AA] + water systems was also determined. The PPG 400 was concentrated in the top phase of the secondary ATPS; this could serve as a means to recover PPG 400 from the primary ATPS via the formation of secondary ATPS.

1. Introduction

Aqueous two-phase system (ATPS) is a type of liquid-liquid extraction method that has been widely studied for application in purification and separation of biomaterials such as proteins, cell organelles, antibiotics and viruses [1–6]. The conventional ATPS was prepared by mixing aqueous solutions of two incompatible hydrophilic polymers or a polymer and an inorganic salt, above their critical concentrations. The high water content in the ATPS allows the biological activity of biomolecules to be maintained efficiently [7]. Other advantages offered by an ATPS include low interfacial tension, economical for large-scale processes, and ease of scaling-up [4].

However, the poor adoption of the conventional polymer-based ATPSs in industrial applications is attributed to the difficulties in final separation of target products from the polymer-rich phase, and also the recycling of the phase-forming components [8]. In recent years, research interest has been focused on the use of 'smart' polymers in forming ATPSs for practical applications [8–10]. These 'smart' polymers could be recovered easily via precipitation induced by stimuli such as temperature, pH, light, and electric potential [11]. For instance, the solubility of a thermo-responsive polymer in water decreases when the temperature of the polymer solution is raised above a critical temperature, which is known as the lower critical solution temperature (LCST). At the LCST, polymer-rich emulsion droplets are formed, rendering the solution turbid. Eventually, two macroscopic phases consisting of a polymer-rich phase and a water-rich phase separate from the

* Corresponding author at: Chemical Engineering Discipline, School of Engineering, Monash University Malaysia, Jalan Lagoon Selatan, 47500 Bandar Sunway, Selangor, Malaysia.
E-mail address: ooi.chien.wei@monash.edu (C.-W. Ooi).

http://dx.doi.org/10.1016/j.jct.2017.07.028
0021-9614/

turbid solution. In this manner, the phase-forming polymer can be conveniently recovered for the next extraction process.

Poly(propylene glycol) 400 (PPG 400) is a type of thermo-responsive polymer having a LCST at 313.15 K. The structure of PPG is closely related to poly(ethylene glycol) (PEG), which is a type of widely used phase-forming polymer in ATPS [12]. Owing to the relatively more hydrophobic nature, PPG solution has a lower LCST than the PEG solution. In general, the LCST of PEG solution is 368.15 K [13]. Therefore, the recovery of PPG from the PPG-solvent mixture via thermo-separation is more economically viable than that for PEG. For example, the top/bottom phases from a primary ATPS containing PPG 400 can be thermo-induced to form secondary ATPSs. The PPG-rich phase from the secondary ATPSs could be recovered for subsequent use. In addition, the formation of secondary ATPS from the primary phases could serve as a means to further fractionate several target biomolecules in ATPS, thereby enhancing the separation of biomolecules in ATPSs. PPG was found to be biodegradable and nontoxic. Also, the high solubility of low-molecular-mass PPG makes it suitable for the formation of ATPSs with phase-forming components like inorganic salts and ionic liquids (ILs) [14–17]. Hence, PPG emerges as a popular ATPS-forming candidate suitable for the applications demanding environmental friendliness and recyclability. The mechanisms of phase formation of ATPS composed of PPG and ionic liquids were recently disclosed [18].

The potential of cholinium ([Ch])-based ILs as the phase-forming component in ATPSs has been well explored. [Ch]-based ILs with anions derived from perfluoroalkanoate [19], organic acids [20,21], carboxylic acids [22] and others (i.e., formate, acetate, propionate, butyrate, glycolate, lactate, benzoate, oxalate, dihydrogencitrate, citrate, chloride, bicarbonate and dihydrogen phosphate) [15,23] have been successfully used to form ATPS. Recently, [Ch]-based ILs comprising aminoate [AA] anions have been reported as useful for a number of applications [24] and are known to be biologically compatible in benign extraction processes.

Previously, our research group has developed a series of ATPSs composed of PPG 400 and cholinium aminoate ([Ch][AA]) [25]. The separation of proteins in these ATPSs could be made specific because the [Ch][AA] exhibits a broad range of hydrophobicity, depending on the nature of [AA] anion species coupled to the [Ch] cation. We also discovered that the charge of the [AA] anion species in [Ch][AA] is tunable as a function of system pH, which plays an influential role in the partitioning of protein in ATPS [25]. By using an appropriate [AA] anion, the interactions between the phase component and the proteins can be controlled, thereby promoting the selective distribution of a target protein in the ATPS. The phase-forming ability of the [Ch][AA] was proven to be dependent on the hydration capacity of the respective anions.

In this work, LLE data of ATPSs comprising PPG 400 and a series of [Ch][AA]s, which include cholinium lysinate ([Ch][Lys]), cholinium β-alaninate ([Ch][β-Ala]), cholinium glycinate ([Ch][Gly]) and cholinium serinate ([Ch][Ser]), at $T = (288.15$ and $308.15)$ K are presented and compared with the LLE data previously determined at $T = 298$ K [25]. A variant of the Merchuk equation and a nonlinear empirical expression with four fitting parameters were used to correlate the binodal data. The Othmer-Tobias and Bancroft equations were used to validate the tie-line data of the investigated systems. The tie-lines were modeled using a modified symmetric electrolyte nonrandom two-liquid model (e-NRTL) [26] that includes the temperature-dependent binary interaction parameters. Additionally, the Setschenow-type equation was employed to correlate the tie-line data. The formation of secondary ATPSs from the corresponding top phases of primary PPG 400 + [Ch][AA] + water systems was studied, and the liquid-liquid equilibrium (LLE) of secondary ATPSs were then characterized.

2. Experimental

2.1. Materials

Table 1 shows the list of the materials used in this work, together with their sources and purity, respectively. All of these chemicals were used without further purification. The synthesis and characterization of [Ch][AA]s used in this study can be found in Supporting Information. The water content in [Ch][AA]s, as shown in Supporting Information, was accounted for upon the preparation of solution.

2.2. Construction of binodal curves

The binodal curves were determined by a turbidimetric titration method [27]. The defined mass fractions of [Ch][AA], PPG 400 and deionized water were added into a 15-mL centrifuge tube to form a turbid solution. The turbid mixture was maintained at a specific temperature using a thermostatic bath (Alpha RA 8, Lauda). Then, deionized water was added drop-wise into the mixture followed by quick vortexing. The addition of deionized water continued until the turbid solution became clear. By determining the amount of deionized water added to the solution, the mass fractions of [Ch][AA] and PPG 400 at the phase-transition point can be calculated. The point data were then used to plot the binodal curve.

2.3. Determination of tie lines

The tie-line data were obtained from the compositions of both top and bottom phases of the investigated ATPSs. In brief, the ATPS was prepared by loading the appropriate amounts of [Ch][AA], PPG 400 and deionized water into a 2-mL micro-centrifuge tube. The micro-centrifuge tube was then incubated in a thermostatic bath at a desired temperature for 2 h to ensure a complete phase separation. After attaining the phase equilibrium/separation, samples from both phases were carefully withdrawn. The UV absorbance

Table 1
List of chemicals.

Chemical name	Source	Initial mole fraction purity
Choline hydroxide (20.9 wt% in water)	Sigma-Aldrich (Australia)	0.95–1.11
β-alanine	Sigma-Aldrich (Australia)	0.995
L-serine	Sigma-Aldrich (Australia)	0.990
L-lysine	Sigma-Aldrich (Australia)	0.980
Glycine	Merck (Australia)	0.990
PPG (446 g mol^{-1})	Sigma-Aldrich (USA)	0.995
[Ch][β-Ala]	Synthesized in-house	0.954
[Ch][Ser]	Synthesized in-house	0.972
[Ch][Lys]	Synthesized in-house	0.952
[Ch][Gly]	Synthesized in-house	0.949

of samples were then measured at 277 nm using a spectrophotometer (Cary 100 UV–Vis, Agilent Technologies). The wavelength 277 nm was selected for the quantification of [Ch][AA] based on the wavelength screening and interference test (see Fig. S5 and Table S1 in Supporting Information). The concentration of [Ch][AA] was calculated using the standard curves for UV absorbance of [Ch][AA] shown in Fig. S6 (in Supporting Information). Next, the samples were vacuum-dried using a freeze dryer (CoolSafe series, ScanVac) operated at 181.15 K for 24 h; the average dried weight was determined gravimetrically [28]. Subsequently, the concentration of PPG 400 was calculated by subtraction of the corresponding [Ch][AA] concentration from the average dried weight of the samples.

2.4. Formation of secondary two-phase systems

The primary PPG 400 + [Ch][AA] + water systems were first prepared at 298.15 K. Next, the (PPG 400)-rich top phase was removed and transferred to a 2-mL micro-centrifuge tube. The micro-centrifuge tube was incubated in a thermostatic bath at 308.15 K. After 2 h of incubation, the homogenous solution was separated into two phases, which are denoted as a 'secondary ATPS' in this study. The concentrations of PPG 400, [Ch][AA] and water in both top and bottom phases of the secondary ATPSs were analyzed using the methods described in Section 2.3.

3. Results and discussion

3.1. LLE data of primary PPG 400 + [Ch][AA] + water systems

The availability of LLE data is crucial for defining the working region of an ATPS [29] for the practical applications such as purification of biomolecules. The LLE data provide information of (i) binodal data, i.e., the concentration of phase-forming components required to form two phases in equilibrium; (ii) the concentrations of phase components in the top and bottom phases. The compositions of the top and bottom phases, which are in thermodynamic equilibrium, are linked by a tie line. The tie-line length (TLL) and the slope of the tie line (STL) were calculated using Eqs. (1) and (2), respectively:

$$\mathrm{TLL} = \left[\left(w_1^t - w_1^b\right)^2 + \left(w_2^t - w_2^b\right)^2\right]^{0.5} \tag{1}$$

$$\mathrm{STL} = \frac{w_1^t - w_1^b}{w_2^t - w_2^b} \tag{2}$$

where w is the mass fraction of phase component; the subscripts '1' and '2' refer to PPG 400 and [Ch][AA], respectively; the superscripts 't' and 'b' refer to top and bottom phases of the system, respectively.

The binodal data, along with the tie-line compositions and TLL and STL, for PPG 400 + [Ch][Lys]/[Ch][Ser]/[Ch][Gly]/[Ch][β-Ala] + water systems were experimentally determined at T = (288.15 and 308.15) K. Literature LLE data for ATPSs at T = 298.15 [25] are also presented for auxiliary illumination. The binodal curves of the investigated systems at different temperatures are shown in Fig. 1 and Table S2 (in Supporting Information). When the temperature increased from 288.15 K to 308.15 K, all the binodal curves were located closer to the origin. This indicated that the formation of an ATPS can be facilitated by use of higher temperature conditions. However, in the [Ch][Lys] systems, the positions of the binodal curves at 298.15 K and 308.15 K were nearly identical.

The effect of temperature on the binodal curves of ATPS was noticeably dependent on the type of phase-forming components used. For instance, the binodal curves of polymer + polymer + water systems, or polymer + kosmotropic salt + water systems shifted towards the origin of phase diagram at an increasing temperature; this indicated that a higher temperature was conducive to the formation of ATPS [30,31]. Conversely, the binodal curve of IL + salt + water systems was displaced further from the origin of phase diagram, hinting that the formation of two-phase system was less favourable [32–34]. On the other hand, the binodal curve of ATPSs consisting of a hydrophilic alcohol and salt was hardly influenced by the temperature [35,36]. Here, the effect of temperature on the binodal curves of PPG 400 + [Ch][AA] + water systems showed a good agreement with that of polymer + polymer + water systems, and polymer + kosmotropic salt + water systems.

Table 2 presents the tie-line data for the investigated systems at different temperatures. The decrease in STL is more prominent at 288.15 K and 308.15 K as compared to 298.15 K. In general, at any given temperature, the TLL increased when the total compositions of phase-forming components in ATPS increased. For instance, systems composed of 40 wt% PPG 400 + 9.5 wt% [Ch][Lys] + 50.5 wt% water, 45 wt% PPG 400 + 10.5 wt% [Ch][Lys] + 44.5 wt% water, or 50 wt% PPG 400 + 11.4 wt% [Ch][Lys] + 38.6 wt% water, have a longer TLL at 308.15 K than that at 288.15 K. This indicates that the two-phase region in phase diagram (i.e., above the binodal curve) was expanded by an increase in temperature. The formation of these ATPSs was mainly attributed to the mutual miscibilities of PPG 400 and [Ch][AA] [18]. PPG 400 becomes more hydrophobic with increasing temperature [37], making its interactions with water molecules weaker at a higher temperature. As a result of water migration from the PPG-rich top phase to the [Ch][AA]-rich bottom phase, the concentration of PPG 400 in the top phase increased while the concentration of IL in the bottom phase decreased.

Plait point is a critical point on the binodal curve at where the TTL has decreased to zero, indicating that the composition and volume of two phases become theoretically identical. The estimated plait points for all the investigated PPG 400 + [Ch][AA] + water systems at T = (288.15, 298.15 and 308.15) K are tabulated in Table 2 and illustrated in Figs. S7–S10 (in Supporting Information). Based on the tie-line compositions in phase diagram, an auxiliary straight line was first plotted using a linear equation: [38].

$$w_1 = f + g w_2 \tag{3}$$

where w_1 and w_2 are the mass fractions for PPG 400 and [Ch][AA], respectively, while the f and g represent the fitting parameters. The corresponding plait point was then calculated as the intercept between the extrapolated auxiliary straight line and the binodal curve (i.e., derived from the four-parameter nonlinear expression as a function of temperature). The calculated fitting parameters of Eq. (3) and the corresponding R^2 for all the studied systems are presented in Table S3 (in Supporting Information).

The position of plait point in PPG 400 (1) + [Ch][AA] (2) + water (3) systems at different temperatures is closely related to the STLs. For example, the tie lines from PPG 400 (1) + [Ch][AA] (2) + water (3) systems at T = 298.15 K are nearly parallel as shown in Table 2; the generated auxiliary straight line can therefore pass through the mid-points of all the tie lines, and eventually intersect with the binodal curve at a lower position in the phase diagram. On the other hand, for PPG 400 (1) + [Ch][AA] (2) + water (3) systems at T = (288.15 and 308.15) K, the STLs decreased at an increasing concentration of [Ch][AA]. Thus, the point of intersection between the auxiliary straight line and the binodal curve was found to be at a higher position in the phase diagram.

3.2. Binodal data correlation

A four-parameter nonlinear expression, as shown in Eq. (4), was used to correlate the experimental binodal data obtained in this study.

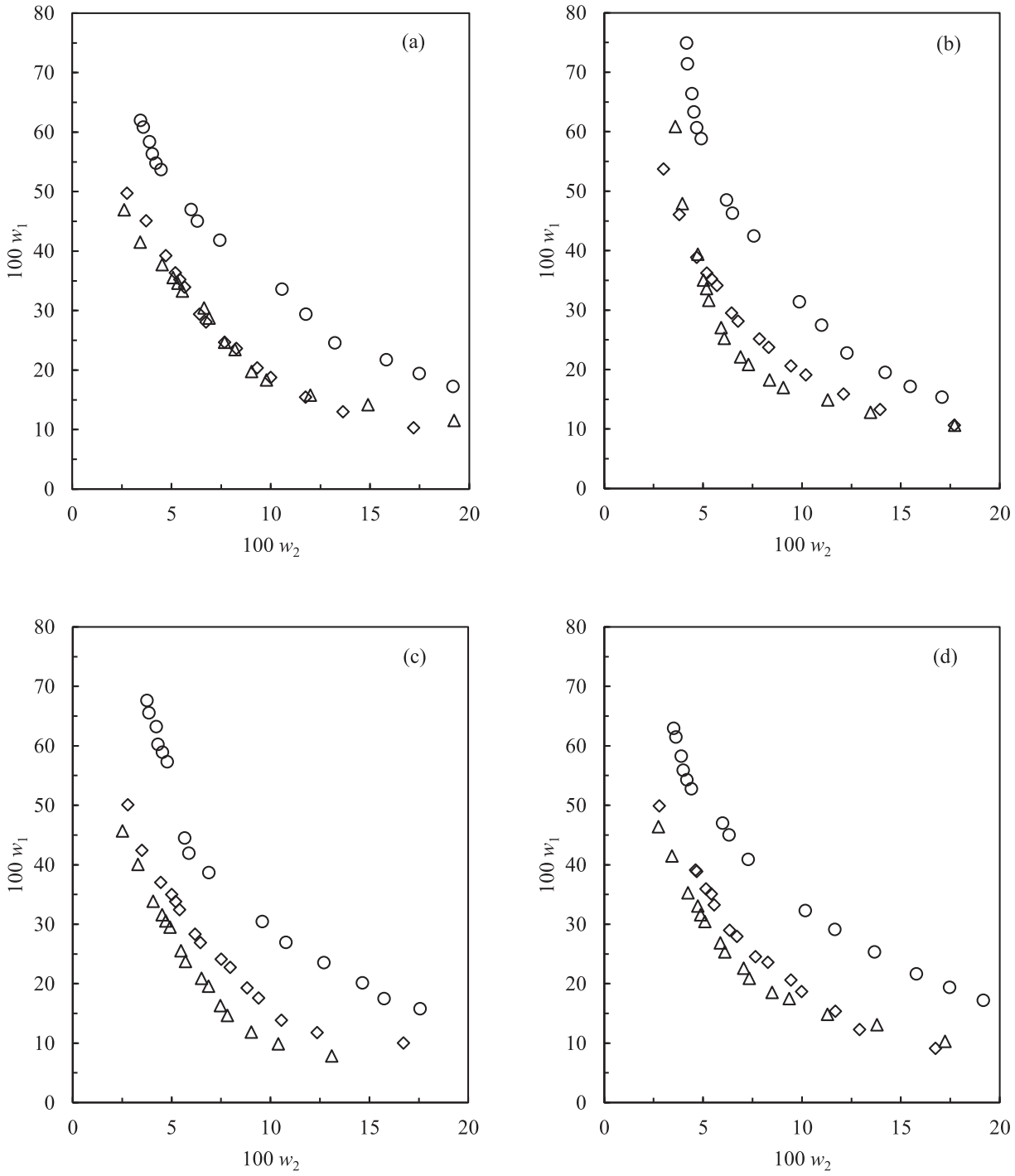

Fig. 1. Binodal curves for PPG 400 (1) + [Ch][AA] (2) + water (3) systems at different temperatures. (a) [Ch][Lys]; (b) [Ch][Ser]; (c) [Ch][Gly]; (d) [Ch][β-Ala]; ○ 288.15 K; ◇ 298.15 K [25]; △ 308.15 K.

$$w_1 = \exp(a + bw_2^{0.5} + cw_2 + dw_2^2) \quad (4)$$

where w_1 and w_2 are the mass fractions of the PPG 400 and [Ch][AA], respectively, while a, b, c and d are the fitting parameters. These equations have been widely used for the correlation of the binodal data of polymer + salt + water [39], IL + salt + water [40], and polymer + IL + water systems [41]; the obtained fitting results were highly satisfactory. To incorporate the temperature dependency in the fitting parameters of Eq. (4), a linear form of each parameter as a function of temperature was adopted [42]. Thus, the four-parameter nonlinear expression was expressed in the forms of Eq. (5),

$$w_1 = \exp([a_0 + a_1|(T - T_0)|] + [b_0 + b_1|(T - T_0)|]w_2^{0.5} + [c_0 + c_1|(T - T_0)|]w_2 + [d_0 + d_1|(T - T_0)|]w_2^2) \quad (5)$$

where T is the absolute temperature and T_0 is the reference temperature (i.e., 298.15 K). The fitting parameters in Eq. (5) was estimated by the least-square regression analysis of experimental binodal data. The values of fitting parameters, along with the associated square of correlation coefficients (R^2) and standard deviations (sd),

Table 2
Experimental tie-line data in mass fraction (w_i, where i = 1 and 2), tie-line length (TLL), slope of the tie-line (STL) and plait point for PPG 400 (1) + [Ch][AA] (2) + water (3) systems at T = (288.15[a], 298.15[a,b] and 308.15[a]) K and pressure (p) = 101.32 kPa[a].

Total composition		Top phase		Bottom phase		100 TLL	STL	Plait point (w_1, w_2)
100 w_1	100 w_2	100 w_1	100 w_2	100 w_1	100 w_2			
PPG 400 + [Ch][Lys] + water								
T = 288.15 K								(67.3, 2.78)
40.0	9.5	74.3	2.7	24.1	13.1	51.2	−4.8	
45.0	10.5	76.1	2.6	17.3	18.9	61.1	−3.6	
50.0	11.4	79.4	2.7	16.3	23.9	66.6	−3.0	
55.0	12.4	83.1	2.6	15.9	27.1	71.5	−2.7	
60.0	13.3	86.3	2.3	15.5	34.3	77.7	−2.2	
T = 298.15 K[b]								(21.2, 9.24)
22.0	10.5	35.8	5.4	11.4	15.2	26.3	−2.5	
29.0	9.5	43.0	4.3	10.2	17.0	35.2	−2.6	
40.0	6.7	48.3	3.4	9.2	19.7	42.4	−2.4	
49.0	5.7	57.5	2.3	8.5	23.2	53.3	−2.3	
50.0	3.8	53.5	2.4	8.7	21.5	48.7	−2.3	
T = 308.15 K								(41.5, 3.75)
30.0	7.6	53.7	2.0	16.2	11.9	38.8	−3.8	
35.0	8.6	59.4	1.5	12.5	16.6	49.2	−3.1	
40.0	9.5	66.4	1.3	11.3	19.4	57.9	−3.1	
45.0	10.5	73.3	1.0	8.3	24.4	69.1	−2.8	
50.0	11.4	80.1	0.9	4.1	30.1	81.4	−2.6	
PPG 400 + [Ch][Ser] + water								
T = 288.15 K								(67.9, 4.37)
40.0	9.7	73.3	4.1	20.9	13.5	53.2	−5.6	
45.0	10.7	76.3	4.0	14.4	17.8	63.5	−4.5	
50.0	11.7	79.5	3.9	10.5	23.7	71.8	−3.5	
55.0	12.6	82.3	3.7	8.3	29.2	78.3	−2.9	
60.0	13.6	86.4	3.6	7.7	34.7	84.7	−2.5	
T = 298.15 K[b]								(17.8, 10.9)
22.0	10.7	30.8	6.3	11.3	16.6	22.1	−1.9	
29.0	9.7	38.9	4.8	9.1	20.5	33.7	−1.9	
40.0	6.8	45.7	3.9	8.3	23.8	42.4	−1.9	
49.0	5.8	54.6	3.0	8.1	27.2	52.5	−1.9	
50.0	3.9	51.7	2.9	8.1	26.2	49.4	−1.9	
T = 308.15 K								(47.8, 4.08)
25.0	6.8	52.1	3.8	19.1	7.80	33.2	−8.2	
30.0	7.8	57.4	3.6	15.4	10.2	42.6	−6.4	
35.0	8.7	64.3	3.4	13.2	13.3	52.0	−5.2	
40.0	9.7	68.1	3.3	10.9	16.8	58.8	−4.2	
45.0	10.7	72.9	3.2	10.2	20.9	65.1	−3.5	
PPG 400 + [Ch][Gly] + water								
T = 288.15 K								(56.0, 4.62)
40.0	9.5	64.4	3.9	21.0	13.3	44.3	−4.6	
45.0	10.4	70.3	3.3	15.4	20.1	57.4	−3.3	
50.0	11.4	75.3	2.8	14.6	24.3	64.5	−2.8	
55.0	12.3	80.1	2.4	14.3	29.5	71.2	−2.4	
60.0	13.3	85.6	1.9	14.3	35.8	79.0	−2.1	
T = 298.15 K[b]								(13.5, 11.7)
22.0	10.4	30.0	6.0	9.2	18.5	24.3	−1.7	
29.0	9.5	41.0	3.8	8.8	21.6	36.8	−1.8	
40.0	6.6	46.5	3.4	7.7	24.6	44.2	−1.8	
49.0	5.7	56.3	2.1	7.2	28.5	55.7	−1.9	
50.0	3.8	53.4	2.2	7.3	26.7	52.2	−1.9	
T = 308.15 K								(41.0, 3.20)
25.0	6.6	53.3	1.9	10.0	10.0	44.0	−5.3	
30.0	7.6	60.1	1.6	7.9	12.9	53.4	−4.7	
35.0	8.5	67.2	1.5	7.7	15.8	61.2	−4.2	
40.0	9.5	72.1	1.5	7.6	18.3	66.7	−3.9	
45.0	10.4	77.3	1.3	7.4	22.4	72.9	−3.3	
PPG 400 + [Ch][β-Ala] + water								
T = 288.15 K								(45.2, 6.13)
40.0	9.5	55.1	4.0	17.5	19.2	40.5	−2.5	
45.0	10.5	60.2	3.5	16.1	24.9	49.0	−2.1	
50.0	11.4	65.2	3.4	15.8	31.2	56.7	−1.8	
55.0	12.4	70.3	3.0	15.2	36.8	64.7	−1.6	
60.0	13.4	75.4	2.8	14.6	44.9	73.9	−1.4	
T = 298.15 K[b]								(12.8, 12.5)
22.0	10.5	31.7	5.9	8.0	18.5	26.8	−1.9	
29.0	9.5	40.3	4.4	6.8	20.9	37.3	−2.0	
40.0	6.7	47.7	3.4	6.4	23.1	45.8	−2.1	
49.0	5.7	57.5	2.0	5.7	26.5	57.3	−2.1	
50.0	3.8	53.8	2.2	5.8	24.6	53.0	−2.2	

(*continued on next page*)

Table 2 (*continued*)

Total composition		Top phase		Bottom phase		100 TLL	STL	Plait point (w_1, w_2)
100 w_1	100 w_2	100 w_1	100 w_2	100 w_1	100 w_2			
T = 308.15 K								(34.0, 4.42)
25.0	6.7	36.6	4.0	18.7	8.60	18.5	−3.9	
30.0	7.6	45.8	2.7	13.6	13.8	34.1	−2.9	
33.0	8.6	50.2	2.3	8.9	19.3	44.6	−2.4	
40.0	8.6	55.4	2.0	6.1	24.1	54.0	−2.2	
45.0	8.6	60.1	1.7	2.2	29.7	64.3	−2.1	

[a] Standard uncertainty of temperature, $u(T)$ = 1 K and pressure $u(p)$ = 0.5 kPa. Expanded uncertainty: for PPG 400 + [Ch][Lys] + water system, Uc are Uc(PPG 400) = Uc([Ch][Lys]) = 0.0023 (95% level of confidence); for PPG 400 + [Ch][Ser] + water system, Uc(PPG 400) = Uc([Ch][Ser]) = 0.0018 (95% level of confidence); for PPG 400 + [Ch][Gly] + water system, Uc(PPG 400) = Uc([Ch][Gly]) = 0.0021 (95% level of confidence); for PPG 400 + [Ch][β-Ala] + water system, Uc(PPG 400) = Uc([Ch][β-Ala]) = 0.0028 (95% level of confidence).

[b] Data taken from literature [25].

Table 3
Values of parameters of Eq. (5), (a_i, b_i, c_i, d_i, where i = 0 and 1) for PPG 400 + [Ch][AA] + water systems at T = (288.15, 298.15 and 308.15) K.

Temperature (K)	a_0	a_1	10^{-2} b_0	b_1	10^{-2} c_0	10^{-2} c_1	d_0	d_1	R^2	sd[a]
PPG 400 + [Ch][Lys] + water										
288.15	0.052	0.518	−0.766	−0.073	0.583	0.786	0.677	−0.068	0.9958	0.789
298.15	3.674	0	78.48	0	−39.86	0	0.008	0	0.9998	0.605
308.15	0.024	0.308	2.142	0.119	−0.462	−4.934	0.293	−0.028	0.9981	0.916
PPG 400 + [Ch][Ser] + water										
288.15	0.075	0.942	−0.019	−0.428	0.429	9.045	−8.995	0.898	0.9812	1.655
298.15	4.756	0	−25.02	0	−12.95	0	0.003	0	0.9996	0.549
308.15	0.042	1.080	0.138	−0.546	−0.126	1.047	0.085	−0.010	0.9621	0.962
PPG 400 + [Ch][Gly] + water										
288.15	0.066	0.827	−0.018	−0.329	0.405	6.388	−5.343	0.533	0.9733	1.492
298.15	4.109	0	33.77	0	−29.39	0	0.006	0	0.9999	0.873
308.15	0.040	0.243	1.022	0.225	−0.141	−9.451	0.254	−0.023	0.9985	0.479
PPG 400 + [Ch][β-Ala] + water										
288.15	0.046	0.454	−0.017	−0.007	0.326	−1.083	0.648	−0.065	0.9979	1.172
298.15	3.972	0	42.81	0	−28.78	0	0.005	0	0.9997	0.611
308.15	0.039	0.459	0.723	−0.022	−0.135	−1.694	0.266	−0.026	0.9823	0.541

[a] $sd = \left[\sum_{i=1}^{n} (w_1^{cal} - w_1^{exp})^2 / n\right]^{0.5}$, where w_1 represents the concentration of PPG 400 (wt%) and n is the number of binodal data.

are shown in Table 3. The R^2 values obtained for Eq. (5) are close to unity, showing satisfactory fitting. Figs. S7–S10 (in Supporting Information) present the visual comparisons of the experimental and the calculated binodal data for PPG 400 + [Ch][AA] + water systems.

3.3. Correlation of tie-line data

The experimental tie-line data was correlated using equations such as Othmer-Tobias, Bancroft, Setschenow-type and e-NRTL.

3.3.1. Othmer-Tobias and Bancroft equations

The consistency of the determined tie-line compositions was ascertained by the correlation of Othmer–Tobias [Eq. (6)] and Bancroft [Eq. (7)] equations [43].

$$\frac{1 - w_1^t}{w_1^t} = \beta_1 \left[\frac{1 - w_2^b}{w_2^b}\right]^n \tag{6}$$

$$\frac{w_3^b}{w_2^b} = \beta_2 \left[\frac{w_3^t}{w_1^t}\right]^r \tag{7}$$

where w is the mass fraction of phase component; the subscripts '1', '2' and '3' refer to PPG 400, [Ch][AA] and water, respectively; the superscripts 't' and 'b' refer to top and bottom phases of the system, respectively; β_1, n, β_2 and r are the fitting parameters. The values of the fitting parameters in Eqs. (6) and (7) for all the investigated systems at T = (288.15 and 308.15) K, along with the associated (R^2) and sd, are given in Table 4. On the basis of the obtained R^2 values, the plot of log $[(1 - w_1^t)/w_1^t]$ against log $[(1 - w_2^b)/w_2^b]$ from Eq. (6) and the plot of log (w_3^b / w_2^b) against log (w_3^t / w_1^t) from Eq. (7) were linear, thereby proving the consistency of the experimental results.

3.3.2. Setschenow-type equation

The phase-forming abilities of [Ch][AA] at different temperatures was investigated based on the salting-out coefficient in the Setschenow-type equation. It is known that the formation of polymer + IL + water system is essentially driven by the salting-out component, which affects the solubility of the non-electrolyte component in the system. The empirical equation of Setschenow is commonly used to evaluate the salting-out effect [14,44]. This equation, as proposed by Hey et al. [45], has also been used to study the salting-out effect on polymer component at different temperatures.

As shown in Eq. (8), the Setschenow-type equation is a two-parameter equation that can be derived from the binodal theory:

$$\ln\left(\frac{m_1^t}{m_1^b}\right) = k_1(m_1^b - m_1^t) + k_2(m_2^b - m_2^t) \tag{8}$$

where m_1 and m_2 represent the molalities of PPG 400 and [Ch][AA], respectively; the superscripts 't' and 'b' refer to top and bottom phases of the system, respectively; k_1 is a parameter relating the activity coefficient of PPG 400 to its concentration; k_2 is the salting-out coefficient.

In this study, the experimental tie-line compositions of PPG 400 + [Ch][AA] + water systems were used to fit the Setschenow-type equation. In Eq. (8), the term $\ln(m_1^t/m_1^b)$ was considered as a

Table 4
Values of fitting parameters in Eqs. (6) (β_1 and n) and (7) (β_2 and r) for PPG 400 + [Ch][AA] + water systems at T = (288.15, 298.15[a] and 308.15) K.

System	T (K)	Othmer-Tobias equation				Bancroft equation			
		β_1	n	R^2	sd [b]	β_2	r	R^2	sd [b]
PPG 400 + [Ch][Lys] + water	288.15	0.111	0.653	0.921	0.017	18.14	1.252	0.948	0.041
	298.15[a]	0.105	1.634	0.991	0.006	3.648	0.599	0.989	0.010
	308.15	0.103	1.106	0.977	0.013	6.384	0.773	0.971	0.033
PPG 400 + [Ch][Ser] + water	288.15	0.113	0.655	0.961	0.014	16.83	1.111	0.967	0.039
	298.15[a]	0.187	1.553	0.993	0.006	2.740	0.631	0.995	0.008
	308.15	0.129	0.796	0.996	0.004	11.30	1.097	0.996	0.010
PPG 400 + [Ch][Gly] + water	288.15	0.108	0.919	0.962	0.016	9.217	1.012	0.978	0.035
	298.15[a]	0.128	1.928	0.989	0.008	2.687	0.518	0.991	0.012
	308.15	0.068	1.173	0.997	0.004	9.118	0.824	0.998	0.012
PPG 400 + [Ch][β-Ala] + water	288.15	0.284	0.750	0.995	0.001	4.803	1.361	0.997	0.010
	298.15[a]	0.061	2.398	0.994	0.005	3.021	0.411	0.993	0.012
	308.15	0.392	0.623	0.995	0.001	4.269	1.424	0.995	0.010

[a] Data taken from literature [25].
[b] $sd = \left[\sum_{i=1}^{n}(w_1^{cal} - w_1^{exp})^2/n\right]^{0.5}$, where w_1 represents the concentration of PPG 400 (wt%) and n is the number of tie-line data.

linear function of the term $(m_2^b - m_2^t)$. The salting-out coefficient, k_2, was determined from the slopes of Setschenow-type plots shown in Fig. S11 (in Supporting Information). The values of k_2, together with the corresponding R^2 and sd values, for PPG 400 + [Ch][AA] + water systems at different temperatures are presented in Table 5. The tie lines reproduced using Eq. (8) are plotted along with the experimental tie lines in Fig. S12 (in Supporting Information). From Table 5, it can be observed that the k_2 values are greater at higher temperature. The increasing k_2 value indicates that the position of the binodal curve shifts towards the origin of the phase diagram, which corresponds to a decrease in the homogenous phase region. The similar observation can also be noted in Fig. 1. Hence, at an increasing temperature, the phase-forming ability of [Ch][AA] becomes higher due to the greater incompatibility between the [Ch][AA] and PPG 400.

3.3.3. e-NRTL

The thermodynamic characteristics of the biphasic systems can be estimated by the correlation of tie-line data with e-NRTL model. In this study, the symmetrical e-NRTL model proposed by Song and Chen [26] was selected to examine the performance of this model in fitting the tie-line data of PPG 400 + [Ch][AA] + water systems. According to the e-NRTL model, the excess Gibbs free energy of the system (G^E) was calculated based on the summation of two contributions, namely a short-range interaction contribution (sr) and a long-range interaction contribution (lr), as shown in Eq. (9):

$$G^E = G^E_{sr} + G^E_{lr} \tag{9}$$

The excess Gibbs free energy for the short-range interaction can be expressed as:

$$\frac{G^E_{sr}}{nRT} = g^E_{sr} = \sum_m X_m \frac{\sum_i X_i G_{im}\tau_{im}}{\sum_i X_i G_{im}} + \sum_c X_c \frac{\sum_{i\neq c} X_i G_{ic}\tau_{ic}}{\sum_{i\neq c} X_i G_{ic}} + \sum_a X_a \frac{\sum_{i\neq a} X_i G_{ia}\tau_{ia}}{\sum_{i\neq a} X_i G_{ia}} \tag{10}$$

with

$$X_i = \frac{n_i}{n} C_i, \qquad i = m, a, c \tag{11}$$

where m is the molecular compounds (PPG 400 and water); c and a are the cation and anions in the solutions, respectively; X_i is the effective mole fraction of each species; n_i is the number of moles of species i; n is the total number of moles in the solution; C_i = 1, for molecular components.

The binary interaction energy parameter (τ_{ij}) was calculated as the function of temperature using the equation proposed by Ko et al. [46] In order to improve the process of parameter searching, the temperature factor was normalized:

$$\tau_{ij} = \Delta g_{ij0} + \Delta g_{ij1} ln\left(\frac{T}{T_r}\right) + \Delta g_{ij2}\left(\frac{T - T_r}{T_r}\right) \tag{12}$$

where T_r is a reference temperature, which is arbitrarily fixed at 298.15 K.

The local binary parameter (G_{ij}) was determined based on the interaction energies:

$$G_{ij} = exp(-\alpha_{ij}\tau_{ij}) \tag{13}$$

where the non-randomness factor parameter (α_{ij}) is set to be 0.2.

Table 5
Values of the salting-out coefficient (k_2), in Eq. (8), for PPG 400 + [Ch][AA] + water systems at T = (288.15, 298.15 and 308.15) K.

System	T (K)	k_2	R^2	sd[a]
PPG 400 + [Ch][Lys] + water	288.15	0.870	0.940	0.259
	298.15	1.867	0.987	0.013
	308.15	2.239	0.997	0.038
PPG 400 + [Ch][Ser] + water	288.15	1.056	0.961	0.361
	298.15	1.319	0.992	0.025
	308.15	1.792	0.950	0.196
PPG 400 + [Ch][Gly] + water	288.15	0.675	0.961	0.214
	298.15	1.160	0.994	0.011
	308.15	1.342	0.945	0.153
PPG 400 + [Ch][β-Ala] + water	288.15	0.361	0.974	0.088
	298.15	1.602	0.989	0.022
	308.15	1.734	0.992	0.084

[a] $sd = \left[\sum_{i=1}^{n}(w_1^{cal} - w_1^{exp})^2/n\right]^{0.5}$, where w_1 represents the concentration of PPG 400 (wt%) and n is the number of tie-line data.

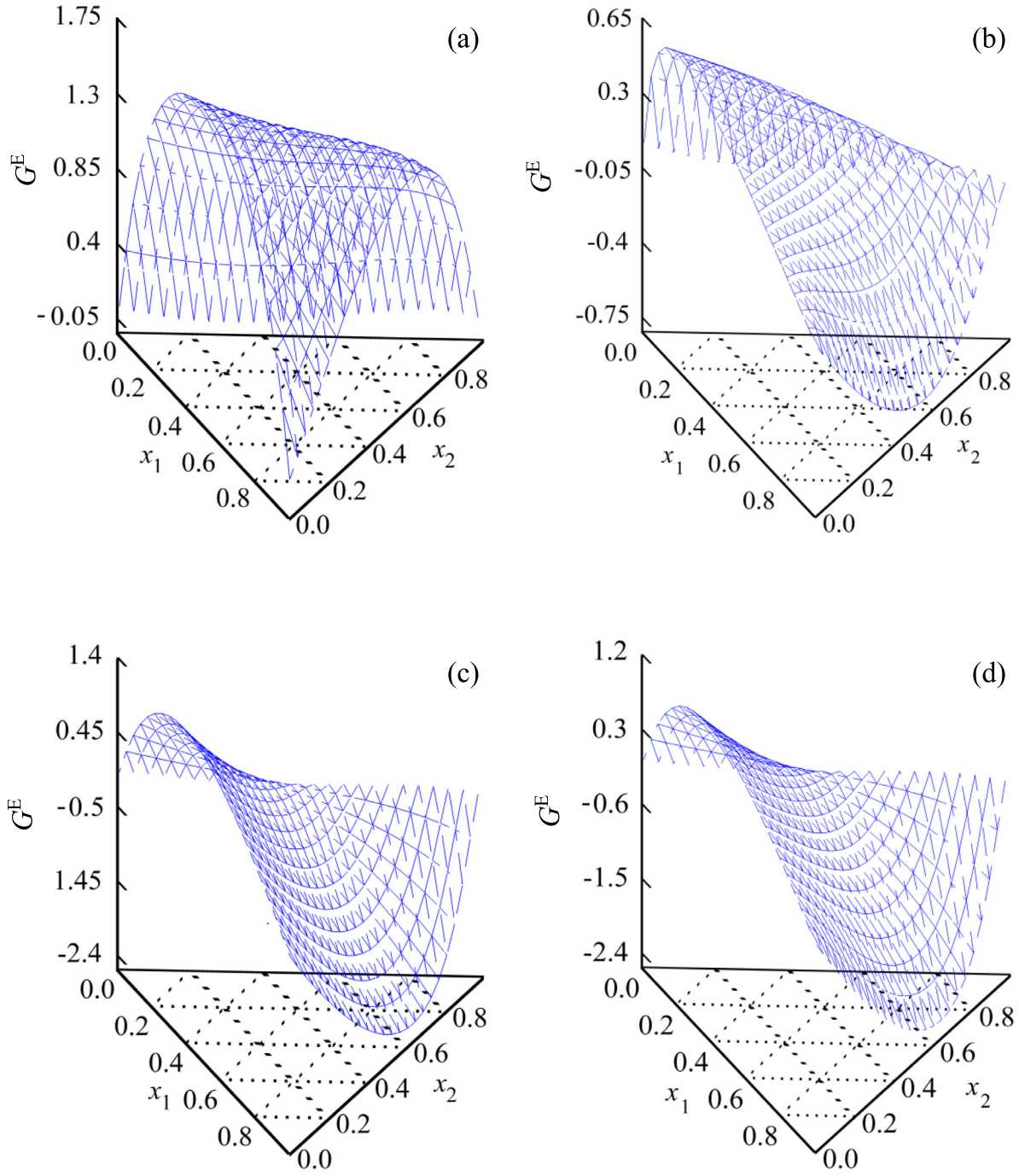

Fig. 2. Plots of the G^E for PPG 400 (1) + [Ch][AA] (2) + water (3) systems at 298.15 K based on e-NRTL model. (a) [Ch][Lys]; (b) [Ch][Ser]; (c) [Ch][Gly]; (d) [Ch][β-Ala]; x_1 and x_2 are the mass fractions of PPG 400 and [Ch][AA], respectively.

The long-range excess Gibbs energy was calculated using the Pitzer-Debye-Hückel (PDH) formula [26,47]:

$$\frac{G^E_{lr}}{nRT} = g^E_{lr} = -\frac{4A_\varphi I_x}{\rho} ln\left[\frac{1+\rho I_x^{1/2}}{1+\rho (I_x^0)^{1/2}}\right] \tag{14}$$

with:

$$A_\varphi = \frac{1}{3}\left(\frac{2\pi N_A}{v}\right)^{1/2}\left[\frac{Q_e^2}{\varepsilon k_B T}\right]^{3/2} \text{ and } I_x = \frac{1}{2}\sum_i x_i z_i^2 \tag{15}$$

where v is the molar volume of the solvent; ε is the dielectric constant (ε =12.5 for PPG 425) [48]; N_A is the Avogadro's number, Q_e is the charge of an electron; ρ is the closest approach parameter (ρ=20); k_B is the Botzmann constant and I_x is the ionic strength.

The activity coefficient of each component (γ_i) can be derived from Eqs. (9), (10) and (14), as shown below:

$$ln\gamma_i = \ln\gamma_i^{sr} + \ln\gamma_i^{lr} = \frac{1}{RT}\left(\frac{\partial G^E_{sr}}{\partial n_i} + \frac{\partial G^E_{lr}}{\partial n_i}\right) \tag{16}$$

Table 6
Values of Δg_{ijk} for PPG 400 (1) + [Ch][AA] (2) + water (3) systems.

i	*j*	*k* = 0	*k* = 1	*k* = 2	*sd*
			Δg_{ijk}		
			PPG 400 + [Ch][Lys] + water		0.023
1	2	9.31	−1559.6	2223.0	
2	1	9.35	7.59	2863.8	
2	3	83.30	18.6	−22.2	
3	2	8.88	25.4	−58.4	
			PPG 400 + [Ch][Ser] + water		0.019
1	2	16.8	−1478.2	1459.4	
2	1	193.2	3557.9	−4357.5	
2	3	−4.8	−13111.0	12638.3	
3	2	10.6	−43799.6	−31031.4	
			PPG 400 + [Ch][Gly] + water		0.019
1	2	8.52	−300.0	350.6	
2	1	0.66	183.8	−131.9	
2	3	−6.5	50.1	−53.9	
3	2	16.2	−0.321	−2.02	
			PPG 400 + [Ch][β-Ala] + water		0.039
1	2	8.8	$-1.08 (\times 10^4)$	10546.4	
2	1	178.9	$-1.32 (\times 10^5)$	139392.8	
2	3	−6.66	−473.2	467.6	
3	2	16.0	3107.3	−3051.9	
			PPG 400 + water		
1	3	−2.23	60.0	−34.6	
3	1	4.43	0.008	58.0	

Note: *i* and *j* are the phase components in the system.

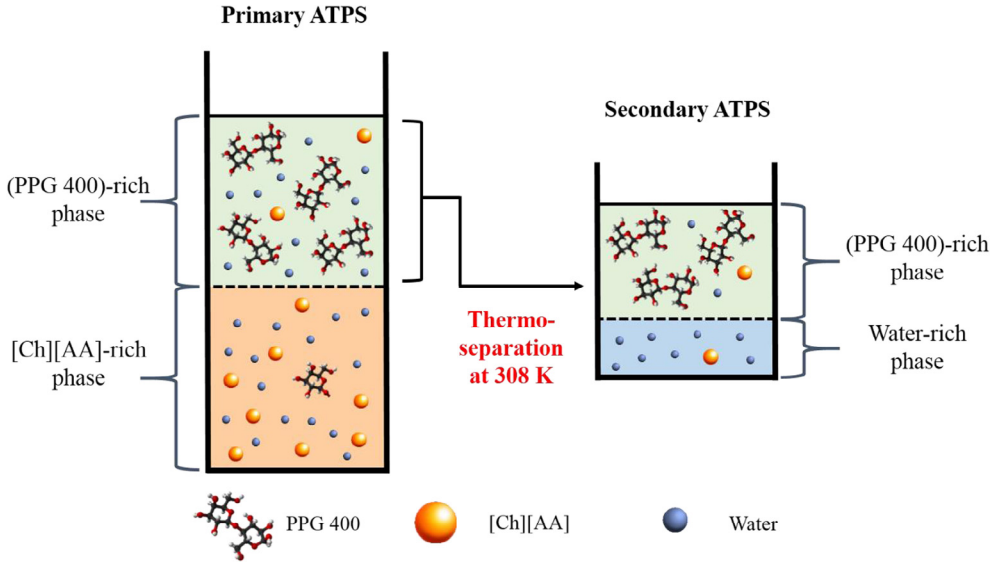

Fig. 3. The secondary ATPSs formed by the thermo-separation of the primary ATPS.

Table 7
Compositions of phase-forming components in secondary ATPSs formed from the top phase of the primary ATPS composing of PPG 400 (1) + [Ch][AA] (2) + water (3) at 308.15 K[a] and *p* = 101.32 kPa[a].

System	Primary top phase[b]		Secondary top phase		Secondary bottom phase	
	100 w_1	100 w_2	100 w_1	100 w_2	100 w_1	100 w_2
50 wt% PPG 400 + 3.8 wt% [Ch][Lys] + 46.2 wt% water	53.5	2.41	82.5	2.01	18.4	2.51
50 wt% PPG 400 + 3.9 wt% [Ch][Ser] + 46.1 wt% water	51.7	2.93	78.2	2.32	19.7	3.32
50 wt% PPG 400 + 3.8 wt% [Ch][Gly] + 46.2 wt% water	53.4	2.23	80.7	1.90	20.3	2.53
50 wt% PPG 400 + 3.8 wt% [Ch][β-Ala] + 46.2 wt% water	53.8	2.23	80.1	1.75	20.5	2.84

[a] Standard uncertainty of temperature, $u(T)$ = 1 K and pressure $u(p)$ = 0.5 kPa. Expanded uncertainty: for PPG 400 + [Ch][Lys] + water system, *Uc* are *Uc*(PPG 400) = *Uc*([Ch][Lys]) = 0.0015 (95% level of confidence); for PPG 400 + [Ch][Ser] + water system, *Uc*(PPG 400) = *Uc*([Ch][Ser]) = 0.0025 (95% level of confidence); for PPG 400 + [Ch][Gly] + water system, *Uc*(PPG 400) = *Uc*([Ch][Gly]) = 0.0017 (95% level of confidence); for PPG 400 + [Ch][β-Ala] + water system, *Uc*(PPG 400) = *Uc*([Ch][β-Ala]) = 0.0023 (95% level of confidence).
[b] Data taken from literature [25].

The details of the development of the symmetric e-NRTL model can be found in the work reported by Song and Chen [26].

The correlation was performed using a two-step method proposed by Espiau et al. [49]. The first step was to minimize the activity difference of each compound in each phase, using the objective function (OF_1) as shown in Eq. (17):

$$OF_1 = \left[\sum_i \sum_j \left(x_{ij}^{I}\gamma_{ij}^{I} - x_{ij}^{II}\gamma_{ij}^{II}\right)^2 / N\right]^{0.5} \quad i = [1,2]; j = [1,\mathrm{N}] \tag{17}$$

Then, the solution obtained in the first step was used as the initial value for the search of the minimum error between the model and the experimental data, represented by the second objective function (OF_2) as follows:

$$OF_2 = \left[\sum_i \sum_j \sum_J \left(x_{ij,exp}^{J} - x_{ij,cal}^{J}\right)^2 / N\right]^{0.5} \quad i = [1,2]; j = [1,\mathrm{N}]; J = [\mathrm{I},\mathrm{II}] \tag{18}$$

Both steps were solved using the Lagarias et al. simplex method [50]. The values of the Δg_{ijk} for each systems, along with their respective *sd* values, are tabulated in Table 5. Overall, an acceptable fit was achieved for all the investigated systems, as shown in Fig. S13 (in Supporting Information), where the calculated tie-line data were in good agreement with the visual comparison of the experimental data. Fig. 2 depicts the surface plots of G^E for PPG 400 + [Ch][AA] + water systems at 298.15 K, based on the values presented in Table 6. It is observed that the G^E values obtained for all the systems are relatively high; this indicates that the formation of ATPS using PPG 400 and [Ch][AA] could be achieved spontaneously.

3.4. Secondary two-phase system LLE data

The temperature-driven phase separation in polymer solution is governed by (i) the balance between hydrophilic and hydrophobic moieties of the polymer chain, (ii) the free energy of mixing, related to the enthalpy, entropy and the temperature of the system [51]. The enthalpy change is associated with the hydrogen bonding of the water molecules surrounding the hydrophobic groups of the PPG 400 and the hydrophobic interactions between the hydrophobic groups present on the polymer chains. Below the LCST, a hydrated cage is formed by the water molecules around the hydrophobic moieties of the polymer chain. As a result, the solvation of the hydrophobic moieties occurs along the polymer chains. However, the increasing entropy of the water molecules with increasing temperature causes desolvation of the hydrophobic moieties and this in turn causes the polymer chains to condense, producing an increase in hydrophobic interactions [52].

In this study, the (PPG 400)-rich top phases originated from the ATPSs (prepared at $T = 298.15$ K) were further thermo-separated into secondary ATPSs at $T = 308.15$ K. Fig. 3 illustrates the formation of secondary ATPS from the top phase of a primary ATPS via thermo-separation. The compositions of the PPG 400 and [Ch][AA] are tabulated in Table 7. The PPG 400 was predominantly concentrated into the secondary top phase but the [Ch][AA] was not one-sidedly partitioned to either of the secondary phases. On the other hand, the primary [Ch][AA]-rich bottom phases were unable to form secondary ATPSs. This was attributed to the low concentration of PPG 400 (5.81–8.72 wt%) [25] in the bottom phase of primary ATPS. Based on the results obtained, the PPG 400 (≈80 wt%) from the secondary top phase could be recovered and recycled for the preparation of a new batch of ATPS.

4. Conclusion

The LLE data for PPG 400 + [Ch][AA] + water systems were determined at $T = (288.15$ and $308.15)$ K. The experimental binodal data were satisfactorily correlated using the four-parameter non-linear expression with a linear form of $(|T - T_0|)$ K as a variable. Good correlations of experimental tie-line data were obtained from the Othmer-Tobias, Bancroft, Setschenow-type and e-NRTL model equations. The salting-out abilities of phase components in PPG 400 + [Ch][AA] + water systems were determined by the Setschenow-type equation, while the e-NRTL model was used to evaluate the thermodynamic of the systems. The Othmer-Tobias equations showed the best fit in the correlation of tie-line compositions of the systems studied. The LLE data of secondary ATPSs were determined, and the PPG 400 was found to be concentrated in the secondary top phase formed at 308.15 K. The formation of secondary ATPS not only offers the possibility of recovering PPG 400 for subsequent preparation of ATPS, but also allows the further partitioning of biomolecules or proteins between the secondary phases formed.

Acknowledgements

This work was funded by the Ministry of Education (MOE) Malaysia under the Fundamental Research Grant Scheme (FRGS) (Ref. no. FRGS/1/2015/SG05/MUSM/02/4), partly developed within the scope of the project CICECO-Aveiro Institute of Materials, POCI-01-0145-FEDER-007679 (FCT Ref. UID/CTM/50011/2013), financed by national funds through the FCT/MEC and when appropriate co-financed by FEDER under the PT2020 Partnership Agreement. The funding support from Tropical Medicine and Biology Platform, Monash University Malaysia, is acknowledged.

Appendix A. Supplementary data

Supplementary data associated with this article can be found, in the online version, at http://dx.doi.org/10.1016/j.jct.2017.07.028.

References

[1] P.L. Show, T.C. Ling, J.C.W. Lan, B.T. Tey, R.N. Ramanan, S.T. Yong, C.W. Ooi, Review of microbial lipase purification using aqueous two-phase systems, Curr. Org. Chem. 11 (2015) 19–29.
[2] Y.K. Lin, C.W. Ooi, R.N. Ramanan, A. Ariff, T.C. Ling, Recovery of human interferon alpha-2b from recombinant *Escherichia coli* by aqueous two-phase system, Sep. Sci. Technol. 47 (2012) 1023–1030.
[3] B. Mokhtarani, R. Karimzadeh, M.H. Amini, S.D. Manesh, Partitioning of Ciprofloxacin in aqueous two-phase system of poly(ethylene glycol) and sodium sulphate, Biochem. Eng. J. 38 (2008) 241–247.
[4] H. Walter, Partitioning in Aqueous Two–Phase System: Theory, Methods, Uses, and Applications to Biotechnology, Elsevier, 2012.
[5] M. Tsukamoto, S. Taira, S. Yamamura, Y. Morita, N. Nagatani, Y. Takamura, E. Tamiya, Cell separation by an aqueous two-phase system in a microfluidic device, Analyst 134 (2009) 1994–1998.
[6] A. Azevedo, P. Rosa, I. Ferreira, A. Pisco, J. De Vries, R. Korporaal, T. Visser, M. Aires-Barros, Affinity-enhanced purification of human antibodies by aqueous two-phase extraction, Sep. Purif. Technol. 65 (2009) 31–39.
[7] M.G. Freire, A.F.M. Claudio, J.M. Araujo, J.A. Coutinho, I.M. Marrucho, J.N.C. Lopes, L.P.N. Rebelo, Aqueous biphasic systems: a boost brought about by using ionic liquids, Chem. Soc. Rev. 41 (2012) 4966–4995.
[8] Y. Wang, Y. Mao, C. Chen, J. Han, L. Wang, X. Hu, T. Chen, L. Ni, Y. Hu, Liquid–liquid equilibrium of aqueous two-phase systems containing thermo-sensitive copolymer L31 and salts, Fluid Phase Equilibr. 387 (2015) 12–17.
[9] L.S. Virtuoso, K.A.S.F. Vello, A.A. de Oliveira, C.M. Junqueira, A.F. Mesquita, N.H. T. Lemes, R.M.M. de Carvalho, M.C.H. da Silva, L.H.M. da Silva, Measurement and modeling of phase equilibrium in aqueous two-phase systems: L35 + sodium citrate + water, L35 sodium tartrate + water, and L35 + sodium hydrogen sulfite + water at different temperatures, J. Chem. Eng. Data 57 (2012) 462–468.
[10] W. Rao, Y. Wang, J. Han, L. Wang, T. Chen, Y. Liu, L. Ni, Cloud point and liquid–liquid equilibrium behavior of thermosensitive polymer L61 and salt aqueous two-phase system, J. Phys. Chem. B 119 (2015) 8201–8208.

[11] A. Kumar, A. Srivastava, I.Y. Galaev, B. Mattiasson, Smart polymers: physical forms and bioengineering applications, Prog. Polym. Sci. 32 (2007) 1205–1237.
[12] S. Hamzehzadeh, M.T. Zafarani-Moattar, Phase separation in aqueous solutions of polypropylene glycol and sodium citrate: effects of temperature and pH, Fluid Phase Equilibr. 385 (2015) 37–47.
[13] M. Iza, G. Stoianovici, L. Viora, J.L. Grossiord, G. Couarraze, Hydrogels of poly (ethylene glycol): mechanical characterization and release of a model drug, J. Control. Release 52 (1998) 41–51.
[14] M.T. Zafarani-Moattar, S. Emamian, S. Hamzehzadeh, Effect of temperature on the phase equilibrium of the aqueous two-phase poly(propylene glycol) + tripotassium citrate system, J. Chem. Eng. Data 53 (2008) 456–461.
[15] Z. Li, X. Liu, Y. Pei, J. Wang, M. He, Design of environmentally friendly ionic liquid aqueous two-phase systems for the efficient and high activity extraction of proteins, Green Chem. 14 (2012) 2941–2950.
[16] A. Salabat, M.H. Abnosi, A.R. Bahar, Amino acids partitioning in aqueous two-phase system of polypropylene glycol and magnesium sulfate, J. Chromatogr. B 858 (2007) 234–238.
[17] E.L. Cheluget, S. Gelinas, J.H. Vera, M.E. Weber, Liquid-liquid equilibrium of aqueous mixtures of poly (propylene glycol) with sodium chloride, J. Chem. Eng. Data. 39 (1994) 127–130.
[18] C.M.S.S. Neves, S. Shahriari, J. Lemus, J.F.B. Pereira, M.G. Freire, J.A.P. Coutinho, Aqueous biphasic systems composed of ionic liquids and polypropylene glycol: insights into their liquid-liquid demixing mechanisms, Phys. Chem. Chem. Phys. 18 (2016) 20571–20582.
[19] D.J. Patinha, L.C. Tomé, C.I.S. Florindo, H. Soares, A.S. Coroadinha, I.M. Marrucho, New low-toxicity cholinium-based ionic liquids with perfluoroalkanoate anions for ABS implementation, ACS Sus. Chem. Eng. 4 (2016) 2670–2679.
[20] X. Liu, Z. Li, Y. Pei, H. Wang, J. Wang, (Liquid + liquid) equilibria for (cholinium-based ionic liquids + polymers) aqueous two-phase systems, J. Chem. Thermodyn. 60 (2013) 1–8.
[21] S. Shahriari, L.C. Tomé, J.M. Araújo, L.P.N. Rebelo, J.A. Coutinho, I.M. Marrucho, M.G. Freire, Aqueous biphasic systems: a benign route using cholinium-based ionic liquids, RSC Adv. 3 (2013) 1835–1843.
[22] T. Mourão, L.C. Tomé, C. Florindo, L.P.N. Rebelo, I.M. Marrucho, Understanding the role of cholinium carboxylate ionic liquids in PEG-based aqueous biphasic systems, ACS Sus. Chem. Eng. 2 (2014) 2426–2434.
[23] J.F. Pereira, F. Vicente, V.C. Santos-Ebinuma, J.M. Araujo, A. Pessoa, M.G. Freire, J.A. Coutinho, Extraction of tetracycline from fermentation broth using aqueous two-phase systems composed of polyethylene glycol and cholinium-based salts, Process Biochem. 48 (2013) 716–722.
[24] Y.-X. An, M.-H. Zong, H. Wu, N. Li, Pretreatment of lignocellulosic biomass with renewable cholinium ionic liquids: biomass fractionation, enzymatic digestion and ionic liquid reuse, Bioresour. Technol. 192 (2015) 165–171.
[25] C.P. Song, R.N. Ramanan, R. Vijayaraghavan, D.R. MacFarlane, E.-S. Chan, C.-W. Ooi, Green, aqueous two-phase systems based on cholinium aminoate ionic liquids with tunable hydrophobicity and charge density, ACS Sus. Chem. Eng. 3 (2015) 3291–3298.
[26] Y. Song, C.-C. Chen, Symmetric electrolyte nonrandom two-liquid activity coefficient model, Ind. Eng. Chem. Res. 48 (2009) 7788–7797.
[27] C.W. Ooi, B.T. Tey, S.L. Hii, A.B. Ariff, H.S. Wu, J.C.W. Lan, R.S. Juang, S.M.M. Kamal, T.C. Ling, Direct purification of *Burkholderia Pseudomallei* lipase from fermentation broth using aqueous two-phase systems, Biotechnol. Bioproc. E. 14 (2009) 811–818.
[28] S. Ramalakshmi, R.N. Ramanan, A.B. Ariff, C.W. Ooi, Liquid–liquid equilibrium of primary and secondary aqueous two-phase systems composed of sucrose + Triton X-114 + water at different temperatures, J. Chem. Eng. Data 59 (2014) 2756–2762.
[29] R. Hatti-Kaul, Aqueous Two-Phase Systems: Methods and Protocols, Springer, 2000.
[30] R. Sadeghi, R. Golabiazar, Thermodynamics of phase equilibria of aqueous poly (ethylene glycol) + sodium tungstate two-phase systems, J. Chem. Eng. Data 55 (2009) 74–79.
[31] K.S. Nascimento, S. Yelo, B.S. Cavada, A.M. Azevedo, M.R. Aires-Barros, Liquid−liquid equilibrium data for aqueous two-phase systems composed of ethylene oxide propylene oxide copolymers, J. Chem. Eng. Data 56 (2011) 190–194.
[32] J. Han, Y. Wang, C. Yu, Y. Li, W. Kang, Y. Yan, (Liquid + liquid) equilibrium of (imidazolium ionic liquids + organic salts) aqueous two-phase systems at T = 298.15 K and the influence of salts and ionic liquids on the phase separation, J. Chem. Thermodyn. 45 (2012) 59–67.
[33] J. Han, Y. Wang, Y. Li, C. Yu, Y. Yan, Equilibrium phase behavior of aqueous two-phase systems containing 1-alkyl-3-methylimidazolium tetrafluoroborate and ammonium tartrate at different temperatures: experimental determination and correlation, J. Chem. Eng. Data 56 (2011) 3679–3687.
[34] C. Sheng, J. Han, Y. Wang, B. Chen, Y. Liu, G. Zhang, Y. Yan, X. Zhao, Liquid–liquid equilibria of ionic liquid 1-(2-methoxyethyl)-3-methylimidazolium bromide + potassium carbonate, potassium phosphate, dipotassium phosphate + water aqueous two-phase systems, Fluid Phase Equilib. 364 (2014) 55–61.
[35] Y. Wang, S. Hu, J. Han, Y. Yan, Measurement and correlation of phase diagram data for several hydrophilic alcohol + citrate aqueous two-phase systems at 298.15 K, J. Chem. Eng. Data. 55 (2009) 4574–4579.
[36] Y. Wang, Y. Mao, J. Han, Y. Liu, Y. Yan, Liquid−liquid equilibrium of potassium phosphate/potassium citrate/sodium citrate + ethanol aqueous two-phase systems at (298.15 and 313.15) K and correlation, J. Chem. Eng. Data 55 (2010) 5621–5626.
[37] R. Sadeghi, Y. Shahebrahimi, Vapor−liquid equilibria of aqueous polymer solutions from vapor-pressure osmometry and isopiestic measurements, J. Chem. Eng. Data 56 (2010) 789–799.
[38] M.T. Zafarani-Moattar, H. Shekaari, P. Jafari, M. Hosseinzadeh, The effect of temperature and molar mass on the (liquid + liquid) equilibria of (poly ethylene glycol dimethyl ether + di-sodium hydrogen citrate + water) systems: experimental and correlation, J. Chem. Thermodyn. 91 (2015) 435–444.
[39] E. Lladosa, S.C. Silvério, O. Rodríguez, J.A. Teixeira, E.A. Macedo, (Liquid + liquid) equilibria of polymer-salt aqueous two-phase systems for laccase partitioning: UCON 50-HB-5100 with potassium citrate and (sodium or potassium) formate at 23 °C, J. Chem. Thermodyn. 55 (2012) 166–171.
[40] J. Han, Y. Wang, C. Chen, W. Kang, Y. Liu, K. Xu, L. Ni, (Liquid + liquid) equilibria and extraction capacity of (imidazolium ionic liquids + potassium tartrate) aqueous two-phase systems, J. Mol. Liq. 193 (2014) 23–28.
[41] M.T. Zafarani-Moattar, S. Hamzehzadeh, S. Nasiri, A new aqueous biphasic system containing polypropylene glycol and a water-miscible ionic liquid, Biotechnol. Progr. 28 (2012) 146–156.
[42] M.T. Zafarani-Moattar, E. Nemati-Kande, Study of liquid–liquid and liquid–solid equilibria of the ternary aqueous system containing poly ethylene glycol dimethyl ether 2000 and tri-potassium phosphate at different temperatures: experiment and correlation, Calphad 34 (2010) 478–486.
[43] D.F. Othmer, P.E. Tobias, Liquid-liquid extraction data-toluene and acetaldehyde systems, Ind. Eng. Chem. 34 (1942) 690–692.
[44] J. Setschenow, Concerning the concentration of salt solutions on the basis of their behaviour to carbonic acid, Z Phys. Chem. 4 (1889) 117.
[45] M.J. Hey, D.P. Jackson, H. Yan, The salting-out effect and phase separation in aqueous solutions of electrolytes and poly (ethylene glycol), Polymer 46 (2005) 2567–2572.
[46] M. Ko, J. Im, J.Y. Sung, H. Kim, Liquid−liquid equilibria for the binary systems of sulfolane with alkanes, J. Chem. Eng. Data 52 (2007) 1464–1467.
[47] C. Mali, S. Chavan, K. Kanse, A. Kumbharkhane, S. Mehrotra, Dielectric relaxation of poly ethylene glycol-water mixtures using time domain technique, Indian J. Pure Appl. Phys. 45 (2007) 476–481.
[48] A.V. Sarode, A.C. Kumbharkhane, Chain length effect on dielectric relaxation and thermo-physical behaviour of organic polymers through relaxation dynamics using TDR, Int. J. Basic Appl. Res. Special Issue (2012) 220–225.
[49] F. Espiau, J. Ortega, L. Fernández, J. Wisniak, Liquid–liquid equilibria in binary solutions formed by [pyridinium-derived][F_4B] ionic liquids and alkanols: new experimental data and validation of a multiparametric model for correlating LLE data, Ind. Eng. Chem. Res. 50 (2011) 12259–12270.
[50] J. Lagarias, J. Reeds, M. Wright, P. Wright, Convergence properties of the Nelder-Mead simplex method in low dimensions, SIAM J. Optim. 9 (1998) 112–147.
[51] M.P. Venkatesh, P.K. Liladhar, T.M.P. Kumar, H.G. Shivakumar, In situ gels based drug delivery systems, Curr. Drug Ther. 6 (2011) 213–222.
[52] M. Bikram, J.L. West, Thermo-responsive systems for controlled drug delivery, Expert Opin. Drug Delivery 5 (2008) 1077–1091.